9-2017

Effects of Wire Material, Deflection, and Interbracket Distance on Burstone Bracket Geometry Force Systems

Skyler J. Liatti

LOMA LINDA UNIVERSITY
School of Dentistry
in conjunction with the
Faculty of Graduate Studies

Effects of Wire Material, Deflection, and Interbracket Distance on Burstone Bracket Geometry Force Systems

by

Skyler J. Liatti

A Thesis submitted in partial satisfaction of
the requirements for the degree
Master of Science in
Orthodontics and Dentofacial Orthopedics

September 2017

Each person whose signature appears below certifies that this thesis in his/her opinion is adequate, in scope and quality, as a thesis for the degree Masters of Science.

_____, Chairperson
Rodrigo F. Viecilli, Associate Professor of Orthodontics and Dentofacial Orthopedics

_____
Joseph Caruso, Professor of Orthodontics and Dentofacial Orthopedics

_____
R. David Rynearson, Associate Professor of Orthodontics and Dentofacial Orthopedics

ACKNOWLEDGEMENTS

I would like to express my gratitude to the late Dr. Charles Bursone and Dr. Herbert Koenig for their contributions to orthodontic biomechanics. Their ingenuity and dedication to scientific truth is second to none and they have been inspirational.

I would like thank my committee chair, Dr. Rodrigo F. Viecilli, for his guidance and support. He consistently directed me while allowing me to find my way to an answer, and more importantly, to the right question. Without his passionate participation and input, this research would not have been possible.

Thank you to the rest of my committee, Dr. Joseph Caruso and Dr. R. David Rynearson for their insightful comments and encouragement.

I would also like to thank my fellow orthodontic students for their feedback, support, and friendship.

Lastly, I would like to thank my family and friends for supporting me throughout writing this thesis, my education, and my life in general. A special thanks to my parents who have always encouraged me to work hard and to never give up.

CONTENT

FIGURES

Figures Page

TABLES

Tables Page

ABBREVIATIONS

PDL	Periodontal Ligament
TMA	Titanium Molybdenum Alloy
IBDr	Interbracket Distance Ratio
θ_A	Angle Bracket A
θ_B	Angle Bracket B
M_y	Moment around y-axis
M	Moment
F	Force
H	Kruskal-Wallis Test Statistic
$\tilde{x}$	Median
IQR	Interquartile Range
SS	Stainless Steel
NiTi	Nickel Titanium
CuNiTi	Copper Nickel Titanium
U	Mann-Whitney Test Statistic
θ_A	Angle Bracket A

ABSTRACT OF THE THESIS

Effects of Wire Material, Deflection, and Interbracket Distance
on Burstone Bracket Geometry Force Systems

by

Skyler J. Liatti

Master of Science, Graduate Program in Orthodontics and Dentofacial Orthopedics
Loma Linda University, September 2017
Dr. Rodrigo F. Viecilli, Chairperson

Objective. This paper aims to quantify the effect of wire material, dimension, and deflection on the most identifiable feature of the six-geometries: the *moment dissociation point* (force system with no moment on the lesser angled bracket), which may or may not occur at the classically defined geometry IV.

Materials and Methods. A six-degree of freedom load cell was used to measure the force systems in different combinations of wire materials, wire dimensions, total angle of bracket, and interbracket distance. Brackets were progressively rotated through Burstone and Koenig's six geometries and the moment on the right bracket was plotted against the ratio of the angle of the two brackets. Regression analysis was used to determine the angular relationship where the actual moment dissociation point occurred for each variable combination. The moment dissociation points were statistically compared.

Results. There were significant differences in the moment dissociation points in the variables studied. A shift in the moment dissociation point toward what is classically considered a geometry III, with lower interbracket distance ratios (*IBDr* = the ratio of distances a) the higher angle bracket to the bracket slot plane intersection and b) total interbracket distance) with linear materials and low wire deflections was observed.

Higher deflections showed a pattern more consistent with the theoretical geometry IV (IBDr 0.33). Superelastic phase transformation at extremely high deflections led to a shift towards a geometry III (lower IBDrs).

Conclusions. The moment dissociation point was not always coincident with a geometry IV as classically defined by Burstone and Koenig. Variables including wire material properties, dimension, and wire deflection affect the location of the moment dissociation point to different extents. The classic geometries as defined by Burstone and Koenig are a simplification of a complex wire deflection problem, especially with phase transforming pseudoelastic wires. In clinical situations, where one is attempting to create or predict the force system on brackets, these data should be taken into consideration, especially to avoid inconsistent force systems.

CHAPTER ONE

INTRODUCTION

The Orthodontic Appliance

Orthodontic appliances are used move teeth through the application of forces and moments.[1,2] Many iterations of the orthodontic appliance have been used for thousands of years. In the modern orthodontic appliance, force systems are produced by engaging a straight wire into a series of attachments (brackets, tubes, buttons, etc.).[1,3] The forces developed when a wire is inserted in two brackets are determined by the angular and step relationships between the bracket of the individual tooth and the wire, as well as the size and shape of both components.[4] It is not always true that, if a wire is bent into the shape in which one would like the brackets to be found at the end of treatment, the teeth will move to that position on the ideal arch and thus produce the desired occlusion.[1] It is the belief of many orthodontists that this is the mechanism by which the straight wire appliance works and it will produce optimal results. This is what is known as a shape driven process and it may lead to tooth alignment, but it may also cause adverse effects such as a canted occlusal plane or a disturbance in arch width.[5] This is because in the process of straightening, the wire applies forces and moments to the teeth which are not necessarily what is required for the tooth to move into its ideal position. A buccally positioned molar may tip adjacent teeth buccally, creating more than optimal overjet for the entire buccal segment. This asymmetry can be difficult and time consuming to correct. Often times, correction requires patient compliance which can introduce further complexity into treatment.

Force Systems

An orthodontic force system consists of forces and moments produced by deflection of the archwire that are balanced by equal and opposite forces acting on the attachments on the teeth.[1] Newton's first law of motion implies that, after initial periodontal ligament (PDL) deformation, an activated orthodontic appliance is in equilibrium since it is not accelerating.[1,2] Since the orthodontic appliance in the patients mouth is remaining stationary, we can conclude that the sum of the forces and moments in the appliance is zero. In other words, the appliance is in static equilibrium. The static equilibrium principle allows us to solve for unknown forces and moments given measurement of some of the forces in the system. These Force systems in which the forces and moments can be readily calculated are called statically determinate.[1,2] Such force systems can be calculated with a clinical measurement of a single force with a force gauge, and the distance between the attachments.[1] Cantilevers are an example of a statically determinate force system where the force of the cantilever single point attachment can be measured and the two-point coupled attachment moment and force can be calculated. Unfortunately, most two-attachment segments produce statically indeterminate force systems where there are too many unknowns to solve for.[1,2,6-8] Continuous archwires fall into the two-attachment category and thus, their force systems cannot be quantitatively defined, unless moments and forces are simultaneously measured with load cells.[9]

If these force systems are indeterminate and the orthodontist cannot calculate the forces and moments on each tooth during continuous archwire alignment, laboratory data can be used to predict the prescribed force system and prevent or control side effects. If

not controlled, side effects occur often enough that the orthodontist spends substantial time and effort correcting them during treatment.[2,10] A non-passive wire passing through a bracket produces a force system between two teeth in isolation from the rest of the arch.[1] The total qualitative force system for a particular tooth can be found by breaking it up into two force systems, one including each adjacent tooth. Using the tooth distal followed by the tooth mesial to the tooth in question, the forces and moments on the middle tooth are then summed, resulting in the force system in question. By adding up a series of these two-tooth force systems the force system can be found for every tooth in the arch. The two-tooth model makes up the simplest unit for understanding forces used in continuous archwires.[2] Burstone and Koenig found that the force systems of a two-bracket model fell into six qualitative categories or geometries that were useful for predicting tooth movement.[1]

Burstone Two-Bracket Geometries

Burstone and Koenig went on to describe a method by which the force system can be identified clinically, by finding the intersection of the two bracket slot axes, as illustrated in Figure 1. If the intersection lies at infinity (the axes are parallel), a geometry I is defined. If the intersection is outside of the two brackets, and they are not parallel, a geometry II exists. A geometry III occurs when the intersection occurs at a bracket. If the intersection is at one third of the interbracket distance, a geometry IV, or moment dissociation point, occurs and the moment on the bracket closest to the intersection point becomes zero. A geometry V occurs next, with the moment that was zero now changing direction, as the intersection point approaches the middle of the interbracket distance. A

geometry VI is when the bracket slot axes cross exactly between the two brackets. The creators of this simplified system to predict tooth movement went on to refine the theoretical two-bracket geometries in their paper dealing with large deflection considerations. They found that whether or not the wire was free to slide in the bracket slot was a more influential variable in determining the force systems in each geometry and concluded that small and large deflection force systems were somewhat similar if the wire was free to slide.[11]

These relationships were also found in studies that aimed to predict tooth movement based on interbracket wire bends.[4,10] Since the force systems in a two-bracket system are generated by wire deflection patterns relative to a bracket slot, the types of force systems are consistent between v-bend, z-bend, and bracket orientation studies.[11] Z-bends produce force systems similar to a geometry I regardless of their location in the interbracket space. V-bends can produce force systems ranging from a geometry IV to VI depending on the location of the v-bend. Geometries II and III force systems are produced with z-bend and v-bend combinations in the interbracket space.

Other Studies

So far, analyses of force systems produced in a two-bracket system have been limited to linear elastic materials with Quick et al. being the first to investigate the effect of v-bends position in nickel titanium wires on the moment dissociation point. They found that the dissociation point occurred with the v-bend significantly closer to a bracket with nickel titanium when compared with TMA wires.[12] Nickel titanium is important to study, not only because of its ubiquity, but its unique engagement capability, high

resiliency, and production of continuous forces.[13] We know that the force system produced is related to wire deflection patterns and superlastic nickel titanium wires produce deflection patterns different from that of linear elastic materials.[12] Excessive stress within a nickel titanium wire induces a phase transformation from austenite to martensite crystals, thus reducing the stiffness of the wire in a specific area, which leads to more deformation in this same area as the wire deflects.[14,15] The phase transformed areas of the archwire exhibits different mechanical properties and alter the deflection in a manner that, as we hypothesize, affects the force system applied to the teeth.

Purpose of this Study

Since Burstone's classic study, over 40 years ago, little development on the subject of these two-attachment force systems has been made. It has been assumed that the original study is accurate and applicable in clinical situations. The first goal of this study was to reproduce Burstone's findings with newer, more sensitive load cells, to verify his findings for moment dissociation point at a classic geometry IV. Reproducibility is an important part of the scientific process which increases validity of previous research. Secondly, we wanted to determine how the introduction of common variables into the system would affect the moment dissociation point. The variables, which are also present clinically, are wire material, wire dimension, total angle of the brackets, and interbracket distance. Ultimately, this study aimed to verify the moment dissociation point as previously described by Burstone and Koenig, and update it for modern materials so that the clinical orthodontist can better predict the force systems he or she prescribes to each tooth in a continuous ideal arch.

Null Hypothesis

No statistically significant difference exists in the moment dissociation point between different wire materials, dimensions, total angle of brackets, and interbracket distances.

CHAPTER TWO

EFFECTS OF WIRE MATERIAL, DEFLECTION, AND INTERBRACKET DISTANCE ON BURSTONE BRACKET GEOMETRY FORCE SYSTEMS

Skyler J. Liatti, DDS

Orthodontics Student

Loma Linda University School of Dentistry

Orthodontics and Dentofacial Orthopedics

Rodrigo F. Viecilli, DDS, PhD

Associate Professor

Director, Biomechanics and Micro-Imaging Laboratories

Loma Linda University School of Dentistry

Orthodontics and Dentofacial Orthopedics

Joseph Caruso, DDS, MS, MPH

Dean, Program Director, Professor

Loma Linda University School of Dentistry

Orthodontics and Dentofacial Orthopedics

R. David Rynearson, DDS, MS

Associate Professor

Loma Linda University School of Dentistry

Orthodontics and Dentofacial Orthopedics

Abstract

Introduction. Forces applied to the teeth by orthodontic wires are often statically indeterminate and difficult to predict. Burstone and Koenig developed their six-geometries of a two-bracket model to enable clinicians to estimate the force system acting on brackets and recognized additional complexity in large deformation scenarios, which is especially relevant in new orthodontic wires with non-linear properties. This paper aims to quantify the effect of wire material, dimension, and deflection on the most identifiable feature of the six-geometries: the *moment dissociation point* (force system with no moment on the lesser angled bracket), which may or may not occur at the classically defined geometry IV.

Methods. A six-degree of freedom load cell was used to measure the force systems in different combinations of wire materials, wire dimensions, total angle of bracket, and interbracket distance. Brackets were progressively rotated through Burstone and Koenig's six geometries and the moment on the right bracket was plotted against the ratio of the angle of the two brackets. Regression analysis was used to determine the angular relationship where the actual moment dissociation point occurred for each variable combination. The moment dissociation points were statistically compared.

Results. There were significant differences in the moment dissociation points in the variables studied. A shift in the moment dissociation point toward what is classically considered a geometry III, with lower interbracket distance ratios (*IBDr* = the ratio of distances a) the higher angle bracket to the bracket slot plane intersection and b) total interbracket distance) with linear materials and low wire deflections was observed. Higher deflections showed a pattern more consistent with the theoretical geometry IV

(IBDr 0.33). Superelastic phase transformation at extremely high deflections led to a shift towards a geometry III (lower IBDrs).

Conclusions. The moment dissociation point was not always coincident with a geometry IV as classically defined by Burstone and Koenig. Variables including wire material properties, dimension, and wire deflection affect the location of the moment dissociation point to different extents. The classic geometries as defined by Burstone and Koenig are a simplification of a complex wire deflection problem, especially with phase transforming pseudoelastic wires. In clinical situations, where one is attempting to create or predict the force system on brackets, these data should be taken into consideration, especially to avoid inconsistent force systems.

Introduction and Review of the Literature

Orthodontic appliances are used to apply forces and moments to teeth.[1,2] In the modern orthodontic appliance, force systems are produced by engaging a wire into a series of attachments (brackets, tubes, buttons, etc.).[1,3] The forces developed when a wire is inserted in two brackets are determined by the angular and step relationships between the bracket of the individual tooth and the wire, as well as the size and shape of both components.[4] It is not always true that, if a wire is bent into the shape in which one would like the brackets to be found at the end of treatment, the teeth will move to that position on the ideal arch and thus produce the desired occlusion.[1] This shape driven process may lead to tooth alignment, but it may also cause adverse effects such as a canted occlusal plane or a disturbance in arch width.[5]

An orthodontic force system consists of forces and moments produced by deflection of the archwire that are balanced by equal and opposite forces acting on the attachments on the teeth.[1] Newton's first law of motion implies that, after initial periodontal ligament (PDL) deformation, an activated orthodontic appliance is in equilibrium since it is not accelerating.[1,2] Force systems in which the forces and moments can be readily calculated are called statically determinate.[1,2] Such force systems can be calculated with a clinical measurement of a single force with a force gauge, and the distance between the attachments.[1] Cantilevers are an example of a statically determinate force system where the force of the cantilever single point attachment can be measured and the two-point coupled attachment moment and force can be calculated. Unfortunately, most two-attachment segments produce statically indeterminate force systems where there are too many unknowns to solve for.[1,2,6-8] Continuous archwires fall

into the two-attachment category and thus, their force systems cannot be quantitatively defined, unless moments and forces are simultaneously measured with load cells.[9]

If these force systems are indeterminate and the orthodontist cannot calculate the forces and moments on each tooth during continuous archwire alignment, laboratory data can be used to prevent or control side effects. If not controlled, side effects occur often enough that the orthodontist spends substantial time and effort correcting them during treatment.[2,10] A non-passive wire passing through a bracket produces a force system between two teeth in isolation from the rest of the arch.[1] By adding up a series of these two-tooth force systems the force system can be found for every tooth in the arch. The two-tooth model makes up the simplest unit for understanding forces used in continuous archwires.[2] Burstone and Koenig found that the force systems of a two-bracket model fell into six qualitative categories or geometries that were useful for predicting tooth movement.[1]

Burstone and Koenig went on to describe a method by which the force system can be identified clinically, by finding the intersection of the two bracket slot axes, as illustrated in Figure 1.

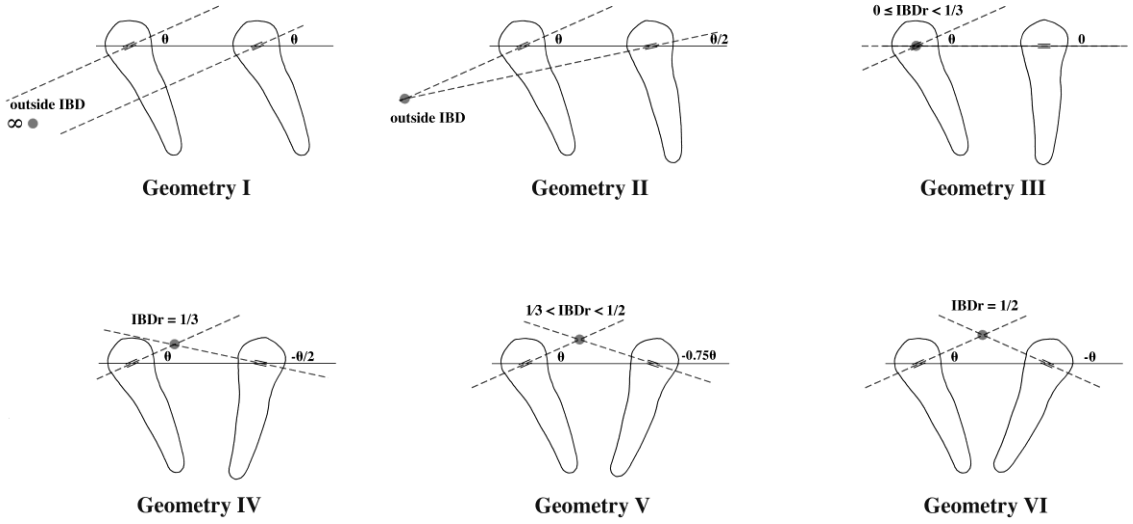

Figure 1. Classic Bursone and Koenig two-bracket geometries.

If the intersection lies at infinity (the axes are parallel), a geometry I is defined. If the intersection is outside of the two brackets, and they are not parallel, a geometry II exists. A geometry III occurs when the intersection occurs at a bracket. If the intersection is at one third of the interbracket distance, a geometry IV, or moment dissociation point, occurs and the moment on the bracket closest to the intersection point becomes zero. A geometry V occurs next, with the moment that was zero now changing direction, as the intersection point approaches the middle of the interbracket distance. A geometry VI is when the bracket slot axes cross exactly between the two brackets. The creators of this simplified system to predict tooth movement went on to refine the theoretical two-bracket geometries in their paper dealing with large deflection considerations. They found that whether or not the wire was free to slide in the bracket slot was a more influential variable in determining the force systems in each geometry and concluded that small and large deflection force systems were somewhat similar if the wire was free to slide.[11]

These relationships were also found in studies that wanted to predict tooth movement based on interbracket wire bends.[4,10] Since the force systems in a two-bracket system are generated by wire deflection patterns relative to a bracket slot, the types of force systems are consistent between v-bend, z-bend, and bracket orientation studies.[11]

So far, analyses of force systems produced in a two-bracket system have been limited to linear elastic materials with Quick et al. being the first to investigate the effect of v-bends position in nickel titanium wires on the moment dissociation point. They found that the dissociation point occurred with the v-bend significantly closer to a bracket with nickel titanium when compared with TMA wires.[12] Nickel titanium is important to study, not only because of its ubiquity, but its unique engagement capability, high resiliency, and production of continuous forces.[13] We know that the force system produced is related to wire deflection patterns and superlastic nickel titanium wires produce deflection patterns different from that of linear elastic materials.[12] Excessive stress within a nickel titanium wire induces a phase transformation from austenite to martensite crystals, thus reducing the stiffness of the wire in a specific area, which leads to more deformation in this same area as the wire deflects.[14,15] The phase transformed areas of the archwire exhibits different mechanical properties and alter the deflection in a manner that, as we hypothesize, affects the force system applied to the teeth.

This study aims to compare the effect of wire material properties, dimension, and deflection on the moment dissociation point, as defined by Burstone and Koenig, using a simple two-bracket model.

Materials and Methods

Experimental Setup

A 0.018x0.025-inch slot, zero prescription, stainless steel orthodontic bracket was mounted to an ATI Nano 17 Titanium six-axis force/moment load cell with piezoresistive transducers (Apex, NC) as depicted in Figure 2.

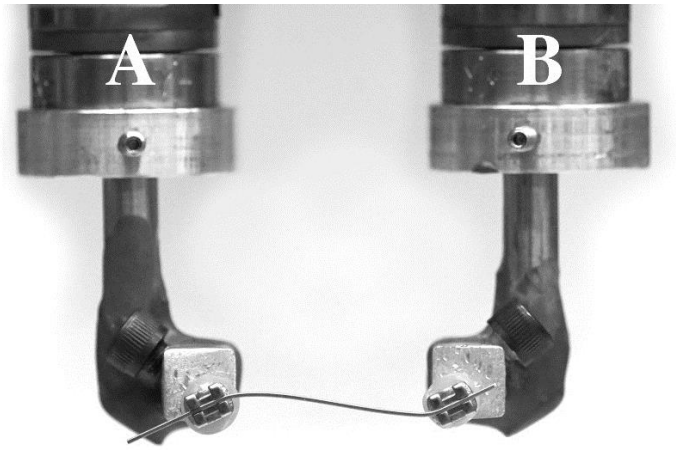

Figure 2. Brackets mounted in geometry I orientation with wire in place.

The load cell was connected to a National Instruments NI USB-6229 DAQ device (Austin, TX) which transferred voltage data to ATI DAQ software (Apex, NC) running on Windows XP. A second orthodontic bracket was mounted at 21 mm distance (on center) in the same bracket slot plane. 21 mm and 7 mm interbracket distances were chosen for anatomical reasons and for comparison with the classic model. The load cell was calibrated so the center of the bracket slot represented the origin of the Cartesian coordinate system with the y-plane perpendicular to the face of the bracket and the x-plane parallel to the bracket slot as illustrated in Figure 3.

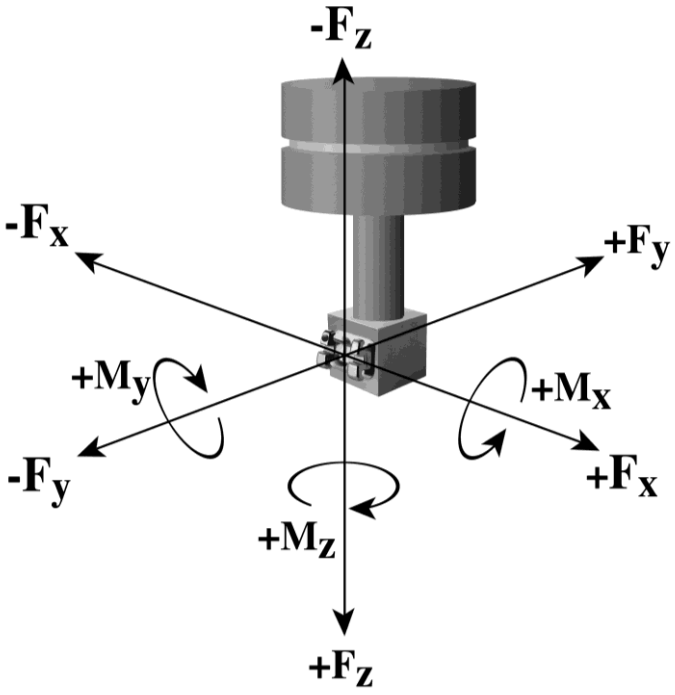

Figure 3. Force/moment load cell calibration coordiate system.

Calibration was carried out by orienting the setup so that the load cell's desired y-axis was parallel to true vertical. The load cell was biased in the software and a weight was hung from the desired origin (center of the bracket slot) so that a pure gravitational force was applied. Force and moment measurements were recorded. Using the rotation equation correlating to an applied y direction force in Table 1, the rotational transformation around the x-axis was calculated and entered into the software calibration transformation matrix. With the new transformation matrix, updated force/moment measurements were acquired and applied to the equation and the transformation matrix was updated with the new result. This was repeated until the calculated angle in the equations reached $0 \pm 0.5°$.

Table 1. Load cell calibration equations.

Applied force direction	*Rotation equation*	*Translation equation*	*Transformation axis*
y	$\theta = \frac{180}{\pi}\left[\cos^{-1}\left(\frac{\lvert F_y\rvert}{\sqrt{F_y^2 + F_z^2}}\right)\right]$	$mm = \frac{M_z}{F_y}$	x
z	$\theta = \frac{180}{\pi}\left[\cos^{-1}\left(\frac{\lvert F_z\rvert}{\sqrt{F_z^2 + F_x^2}}\right)\right]$	$mm = \frac{M_x}{F_z}$	y
x	$\theta = \frac{180}{\pi}\left[\cos^{-1}\left(\frac{\lvert F_x\rvert}{\sqrt{F_x^2 + F_y^2}}\right)\right]$	$mm = \frac{M_y}{F_x}$	z

F, force; M, moment

Next, the setup was oriented so the load cell's desired z-axis was parallel to true vertical. The above process was repeated using the second rotation equation in Table 1 and the rotational transformation around the y-axis was updated until the resultant angle reached $0 \pm 0.5°$. Lastly, the setup was oriented where the load cell's desired x-axis was parallel to true vertical and repeated for the z-axis transformation.

After calibration of rotations around the x,y, and z axes, translation calibration was performed to position the origin of the coordinate system coincident with the center of the bracket slot. The setup was returned to an orientation with the load cell's desired y-axis parallel to true vertical. The software was biased, a weight hung from the desired origin, and force/moment data acquired. The first transformation equation in Table 1 for translation was used to calculate the required displacement along the x-axis. The calculated translation was applied to the software transformation matrix. This was repeated for the x-axis until the resulting displacement calculated reached 0 ± 0.5 mm. The setup was reoriented so the desired z-axis of the load cell was parallel to true vertical. The above translational transformation was then repeated to calibrate the origin

along the y-axis. Finally, the setup was oriented so the load cell's desired x-axis was parallel to true vertical and the z-axis translation was calculated and applied to the matrix.

The above process of calibrating rotation around the x,y, and z axes followed by translation along the x,y, and z axis was repeated, in order, until each resultant calculation produced an output of $0 \pm 0.5°$ and 0 ± 0.5 mm respectively. At this point the load cell setup had been calibrated such that the origin was in the center of the bracket slot and the Cartesian coordinate system was orthogonal to the bracket slot plane.

Both brackets had freedom of rotation around the y-axis and the interbracket distance was adjustable. Ambient temperature was kept between 37.5 and 39.5 degrees C and monitored with an Air Thermapen® (Salt Lake City, UT) instant thermometer.

The left bracket was designated bracket A and the right bracket B. A 0.05-degree resolution General Tools 826 professional digital protractor (Secaucus, NJ) with a 0.018-inch round wire mounted to the center of rotation was used to set bracket angles. Both brackets were rotated counter clockwise around the y-axis to an initial angle (θ_A and θ_B). This represents a geometry I and the starting point for all sets of measurements (Figure 4).

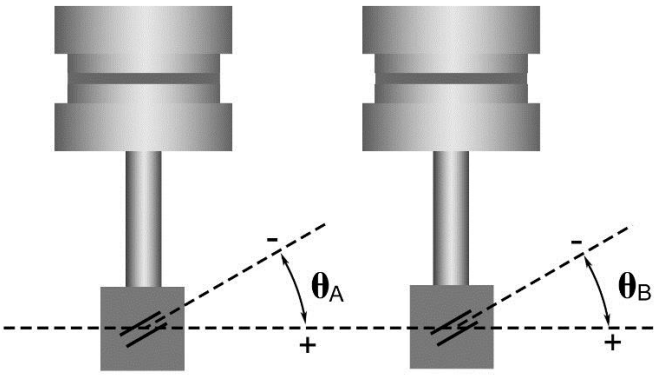

Figure 4. Initial angular relationship of brackets (geometry I).

The load cell software was configured to sample the voltage at 10,000 Hz averaging every 1,000 samples, producing an actual sample refresh rate of 0.1 seconds. The load cell was biased in the software and a straight section of orthodontic wire was inserted into the two bracket slots. A couple and force was applied to the load cell by the wire in the slot which caused distortion of the load cell and a voltage change. The voltage change was transmitted to the software and converted to Newtons of force in three planes of space and gram millimeter moments around all three axes. The forces and moments for bracket B were recorded. After wire removal, the load cell was re-biased, to zero to minimize the hysteresis effect, and the next wire was inserted into the brackets and the process was repeated. A repeat of 10 individual orthodontic wires was used for each setup variable combination.

After all 10 wires were measured, bracket B was rotated clockwise by $1/6^{th}$ of the original counterclockwise rotation and data was collected for all 10 wires. This was incrementally repeated until the bracket B was rotated to same angular magnitude but opposite direction of bracket A, representing a geometry VI.

The above process was repeated for every combination in Table 2.

Table 2. Combinations of wire material, wire size, interbracket distance, and total angle compared.

IBD	Material	0.012”	0.016”	0.016” x 0.022”
21 mm	SS	12°	6°	6°
	TMA	*	12°	12°
	NiTi	24°, 48°	12°, 24°, 48°	12°, 24°, 48°
	CuNiTi	*	12°, 24°, 48°	12°, 24°, 48°
7 mm	SS	‡	6°	†
	TMA	*	6°, 12°	6°
	NiTi	24°	12°	12°
	CuNiTi	*	12°	12°

IBD, interbracket distance; SS, stainless steel; TMA, titanium molybdenum alloy; NiTi, nickel titanium; Cu, 35° copper nickel titanium; * material not available; † material too stiff for IBD; ‡ excessive play

After a two-week burnout period, a random sampling of 33% repeat measurements of each combination were taken for an intraclass correlation analysis.

Analysis

θ_B/θ_A vs. M_y (moment around the y-axis) of bracket B was plotted for the ten wire repeats for each combination. Interpolation of the x-intercept (θ_B/θ_A relationship where the moment on bracket B = 0, also known as the moment dissociation point) was conducted with a regression model for each curve.

Moment dissociation values were imported into SPSS statistical package version 23 (SPSS Inc, Chicago, IL). A Kruskal-Wallis H test, α=0.05, was conducted for each of the variables containing 3 or more groups followed by a post hoc pairwise comparisons using Dunn’s test with Bonferroni correction, α=0.05. A Mann-Whitney U test, α=0.05, was conducted on the variable with two groups. A sensitivity analysis was conducted on the wire material variable, the only variable with an outlier, by removing the outlier from the data set and repeating the Kruskal-Wallis H test and post hoc tests.

Effect size of each variable was calculated with the obtained H-statistic using the following formula: $\eta_H^2 = \frac{H-k+1}{n-k}$, where *k* was the number of groups and *n* was the total number of observations.

The IBDr (Interbracket distance ratios) were calculated using the following equation for each median moment dissociation point:

$$IBDr = \frac{\frac{1}{\tan(\theta_A)}}{\frac{1}{\tan(\theta_A)} + \frac{1}{\tan(\theta_B)}}$$

θ_A (radians) converged on zero, θ_B (radians) was calculated using θ_A multiplied by the dissociation point ratios (θ_B/θ_A) which were found experimentally (Figure 5).

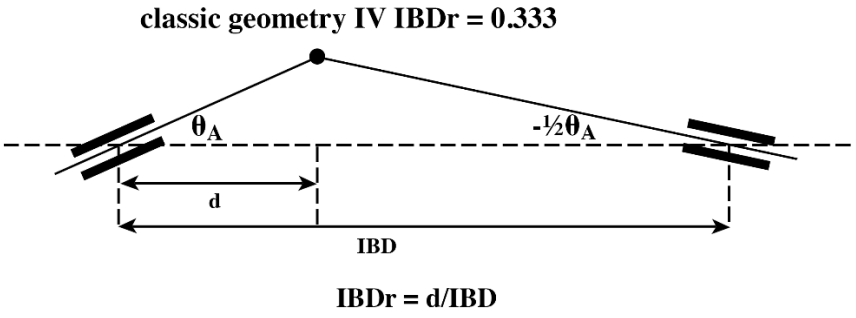

Figure 5. Bracket plane intersection point for a classic geometry IV.

Reliability analysis was conducted by calculating the intraclass correlation coefficient for each group within each variable using repeated data and corresponding original data in SPSS statistical package version 23 (SPSS Inc, Chicago, IL).

Results

A high degree of reliability was found between measurements for all groups. Intraclass correlation coefficients ranged from 0.959 to 0.991 ($p < 0.001$), as described on Table 3.

Table 3. Intraclass correlation analysis for single measures.

			95% Confidence Interval		
Variable	***Group***	***ICC***	***Lower***	***Upper***	***Sig***
Wire Material	SS	**0.991**	0.983	0.993	**<0.001**
	TMA	**0.986**	0.982	0.990	**<0.001**
	NiTi	**0.959**	0.949	0.966	**<0.001**
	CuNiTi	**0.988**	0.984	0.990	**<0.001**
Wire	0.012”	**0.979**	0.970	0.985	**<0.001**
	0.016”	**0.985**	0.982	0.988	**<0.001**
	16x22	**0.974**	0.968	0.978	**<0.001**
Angle Bracket	6°	**0.985**	0.980	0.989	**<0.001**
	12°	**0.984**	0.980	0.987	**<0.001**
	24°	**0.962**	0.951	0.970	**<0.001**
	48°	**0.941**	0.914	0.960	**<0.001**
Interbracket	7 mm	**0.978**	0.972	0.983	**<0.001**
	21 mm	**0.971**	0.966	0.975	**<0.001**

ICC, intraclass correlation coefficient; F, F test statistic; Sig, significance at $\alpha=0.05$; SS, stainless steel; TMA, titanium molybdenum alloy; NiTi, nickel titanium; CuNiTi, 35° copper nickel titanium

Table 4. Descriptive statistics showing median and interquartile range for each variable and group compared.

Variable	***Group***	***N***	***Median***	***IQR***
Wire Material	SS	40	-0.368	0.119
	TMA	60	-0.418	0.184
	NiTi	110	-0.453	0.083
	CuNiTi	80	-0.438	0.126
Wire Dimension	0.012”	40	-0.444	0.056
	0.016”	120	-0.468	0.104
	16x22	130	-0.406	0.129
Angle Bracket A	6°	50	-0.296	0.076
	12°	130	-0.466	0.100
	24°	60	-0.460	0.065
	48°	50	-0.411	0.102
Interbracket Distance	7 mm	100	-0.384	0.159
	21 mm	190	-0.452	0.093

N, sample size; IQR, interquartile range; SS, stainless steel; TMA, titanium molybdenum alloy; NiTi, nickel titanium; Cu, 35° copper nickel titanium

Table 5. Results of the post hoc pairwise comparisons with Dunn-Bonferroni test and Mann-Whitney U test.

Variable	*Comparison*	*Test statistic*	*Std. Error*	*Sig*
Wire Material*	SS-TMA	-59.133	12.322	**0.003** **0.003**‡
	SS-NiTi	-100.227	15.484	**<0.001** **<0.001**‡
	SS-CuNiTi	-79.925	16.239	**<0.001** **<0.001**‡
	TMA-NiTi	-41.094	3.459	**0.014** **0.017**‡
	TMA-CuNiTi	-20.792	14.322	0.879 0.871‡
	NiTi-CuNiTi	20.302	12.322	0.597 0.708‡
Wire Dimension*	0.012”- 0.016”	10.425	15.311	1.000
	0.012”- 16x22	-40.129	15.163	**0.049**
	0.016”- 16x22	-50.554	10.616	**<0.001**
Angle Bracket A*	6° - 12°	133.609	13.995	**<0.001**
	6° - 24°	153.290	16.058	**<0.001**
	6° - 48°	80.220	16.772	**<0.001**
	12° - 24°	19.681	13.088	0.796
	12° - 48°	-53.389	13.955	**0.001**
	24° - 48°	-73.070	16.058	**<0.001**
IBD†	7 mm – 21 mm	-7.163	678.786	**<0.001**

*Dunn-Bonferroni test; † Mann-Whitney U test; ‡ sensitivity test with outliers removed; IBD, interbracket distance; SS, stainless steel; TMA, titanium molybdenum alloy; NiTi, nickel titanium; Cu, 35° copper nickel titanium; Sig, significance

A Kruskal-Wallis test showed that there was a statistically significant difference in the dissociation point between the different wire materials (H = 44.072, p <0.001), as depicted on Figure 6. A post-hoc pairwise comparison with Dunn-Bonferroni analysis (Table 5) showed that stainless steel ($\tilde{x}$ = -0.368, interquartile range, IQR = 0.119)(Table 4) was significantly different from TMA ($\tilde{x}$ = -0.418, IQR = 0.184, p = 0.003), NiTi ($\tilde{x}$ = -0.453, IQR = 0.083, p <0.001), and CuNiTi ($\tilde{x}$ = -0.438, IQR = 0.126, p <0.001). TMA was significantly different from NiTi (p = 0.017). CuNiTi was not significantly different from TMA (p = 0.879) or NiTi (p = 0.708).

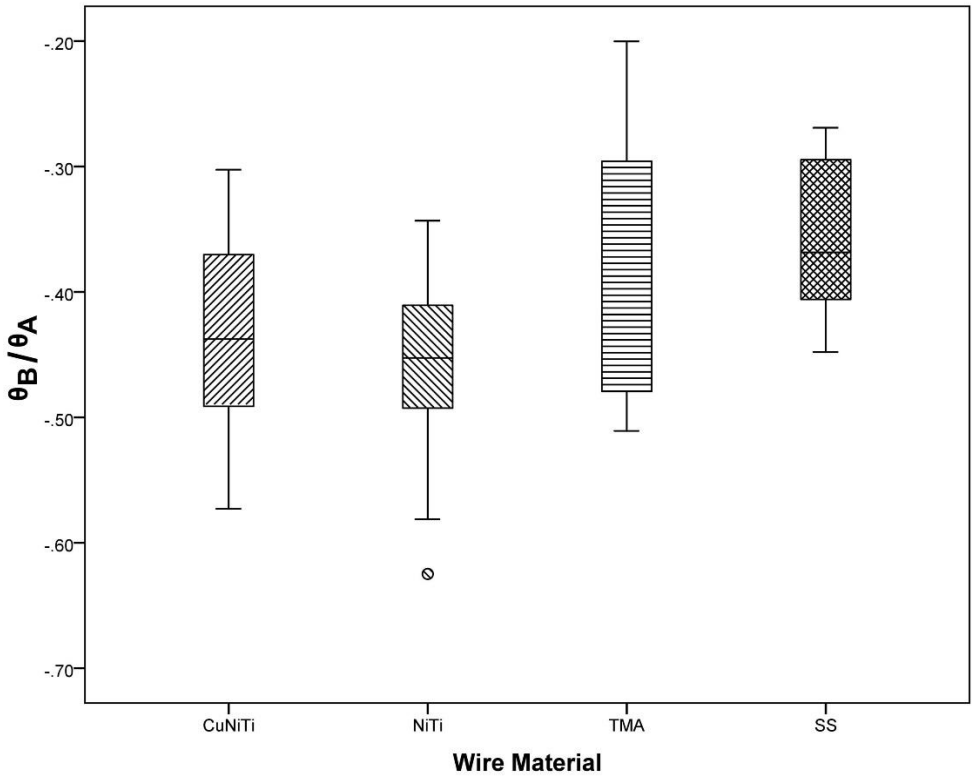

Figure 6. Box plot of bracket B moment dissociation point for different wire materials.

A Kruskal-Wallis test showed that there was a statistically significant difference in the dissociation point between the different wire dimensions (H = 23.911, p <0.001), as shown on Figure 7. A post-hoc pairwise comparison with Dunn-Bonferroni analysis (Table 5) showed that 0.016”x0.022” wire ($\tilde{x}$ = -0.406, IQR = 0.129) was significantly different from 0.012” ($\tilde{x}$ = -0.444, IQR = 0.056, p = 0.049) and 0.016” wire ($\tilde{x}$ = -0.468, IQR = 0.104, p <0.001). The 0.012” diameter wire was not significantly different from 0.016” wire (p = 1.000).

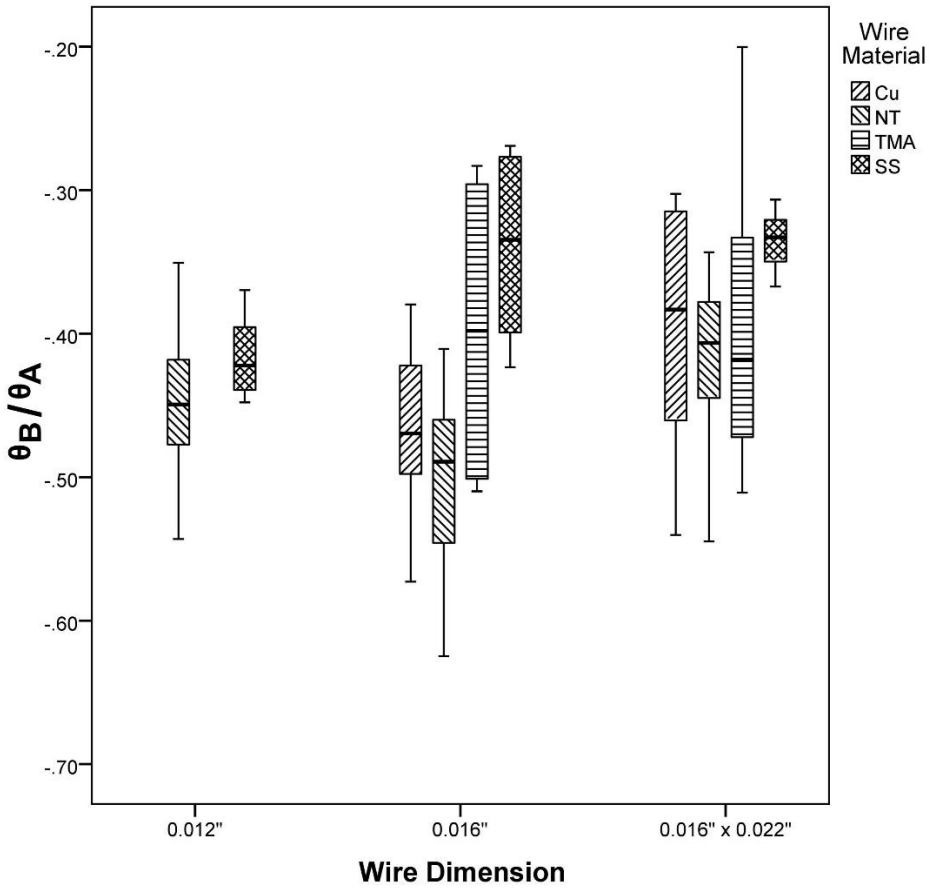

Figure 7. Box plot of bracket B moment dissociation point for different wire dimensions.

A Kruskal-Wallis test showed that there was a statistically significant difference in the dissociation point between the different bracket A angles (H = 117.770, p <0.001), as can be seen on Figure 8. A post-hoc pairwise comparison with Dunn-Bonferroni analysis (Table 5) showed that 6° ($\tilde{x}$ = -0.296, IQR = 0.076) was significantly different from 12° ($\tilde{x}$ = -0.466, IQR = 0.100, p <0.001), 24° ($\tilde{x}$ = -0.460, IQR = 0.065, p <0.001), and 48° ($\tilde{x}$ = -0.411, IQR = 0.102, p <0.001). There was also a significant difference between 48° and both 12° (p = 0.001) and 24° (p <0.001). Bracket A angle of 12° was not significantly different from 24°.

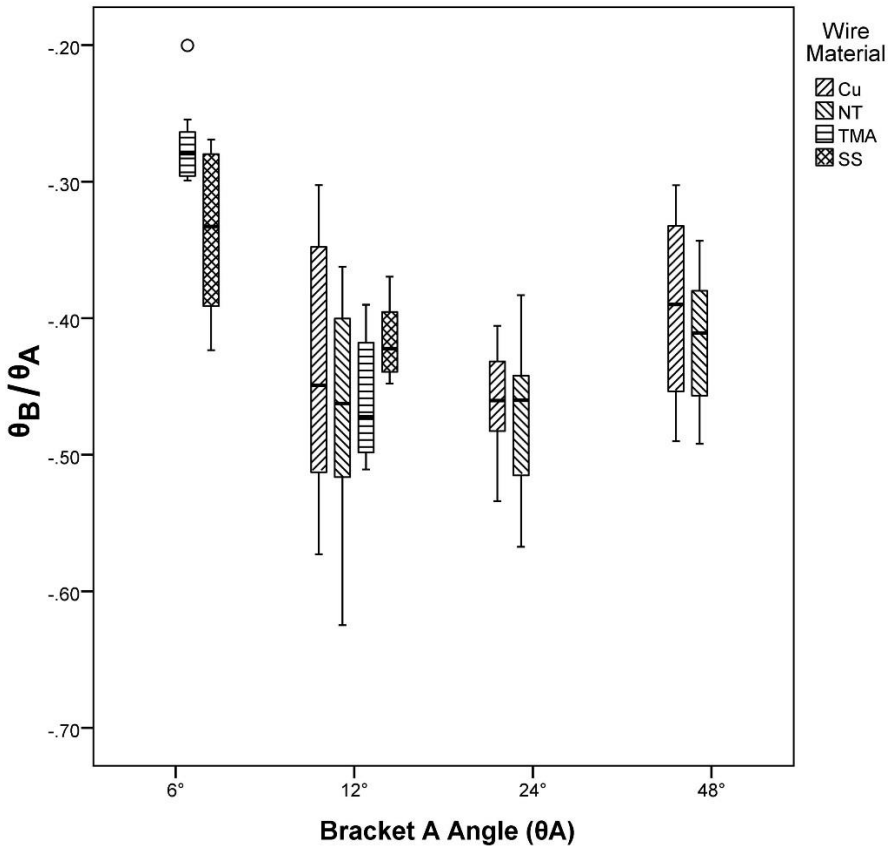

Figure 8. Box plot of bracket B moment dissociation point for different bracket A angles.

A Mann-Whitney U test (Figure 9) indicated that there was a significant difference in the dissociation point between 7mm ($\tilde{x}$ = -0.384, IQR = 0.159) and 21mm ($\tilde{x}$ = -0.452, IQR = 0.093) interbracket distances (U = -7.163, p <0.001)(Table 5).

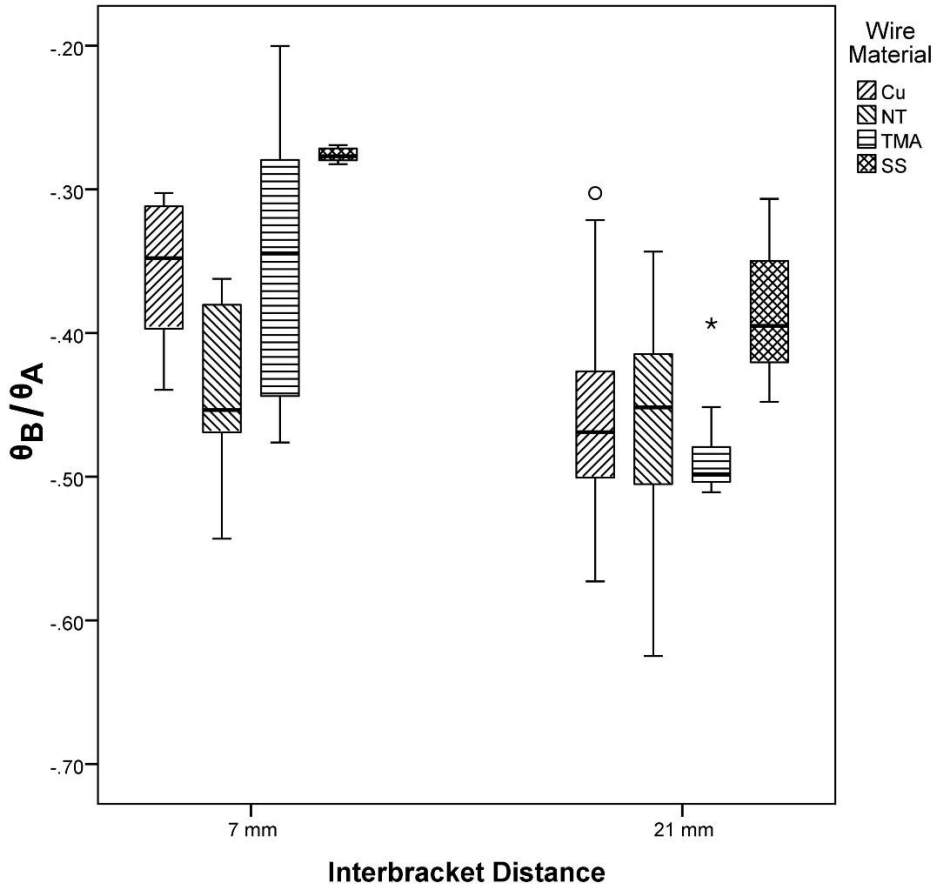

Figure 9. Box plot of bracket B moment dissociation point for different interbracket distances.

Discussion

Burstone and Koenig identified the six two-bracket geometries that could be used to predict initial tooth movement by identifying the angular relationship between the two brackets (Figure 1). The geometries display force system changes in a continuum with one interesting feature, the moment on the lower angle bracket becomes zero and switches directions when it is rotated in the opposite direction one half the angle of the other bracket. They defined this as the moment dissociation point and described its occurrence as a geometry IV. Burstone and Koenig updated their two-bracket geometries when they studied the effects of large deflections and altered the wire sliding through the bracket variable. They found that when the wire is free to slide, small and large defection theories are similar. However, the geometries shift when the wire is no longer free to slide through the brackets. It is important to note that details of the experimental setup used by Burstone and Koenig, such as bracket slot size, or whether clamps (without any wire play) were used, were not provided in their paper. Moreover, statistical treatment of the data was not described, and it is reasonable to believe the accuracy and consistency of the load cell, if used, (not reported in the original paper) was much lower than what is available today.

To study the effect of wire material, size, total angle, and interbracket distance, we used the simplest clinical reduction of an ideal arch, the two-bracket model, to measure the most identifiable landmark within the six geometries, the moment dissociation point. This study modeled a wire that is free to slide through the bracket since the bracket was rotated into the geometry position prior to wire insertion.

Therefore, there were minimal horizontal forces and one would expect results matching the classical model.

The effect of wire material on the dissociation point demonstrated a significant difference between all combinations except for CuNiTi vs NiTi (as expected), and CuNiTi vs TMA. Since TMA stress-strain curve does not follow a perfectly straight line, one can expect it to have a dissociation point somewhere between that of stainless steel and the superelastic materials. The overall pattern was a shift away from the predicted value of moment dissociation in the geometry IV (θ_B/θ_A = -0.5) toward a geometry III (θ_B/θ_A = 0). More elastic materials seem to have a dissociation point closer to Burstone's simplified geometries model, where stiffer materials, such as SS exhibited a shift toward a geotmetry III, which had an interbracket distance ratio (IBDr) of 0.269 (see Table 6).

Table 6. Calculated interbracket distance ratio (IBDr) from median θ_B/θ_A, at the moment dissociation point, for each variable and group compared.
Note: Classic geometry IV (moment dissociation point) IBDr = 0.333

Variable	***Group***	***Median θ_B/θ_A***	***Calculated IBDr***
Wire Material	SS	-0.368	0.269
	TMA	-0.418	0.295
	NiTi	-0.453	0.312
	CuNiTi	-0.438	0.305
Wire Dimension	0.012"	-0.444	0.307
	0.016"	-0.468	0.319
	16x22	-0.406	0.278
Angle Bracket A	6°	-0.296	0.228
	12°	-0.466	0.318
	24°	-0.460	0.315
	48°	-0.411	0.291
Interbracket Distance	7 mm	-0.384	0.277
	21 mm	-0.452	0.311

IBDr, ratio of distance from bracket A to point where bracket plane lines intersect and total interbracket distance; SS, stainless steel; TMA, titanium molybdenum alloy; NiTi, nickel titanium; Cu, 35° copper nickel titanium

IBDr is the ratio of the distances from the point of intersection of the two bracket planes to the higher angle bracket and the total interbracket distance, as can be seen in Figure 5. The IBDr for a classical geometry IV is 1/3 the total IBD. The observed change related with stiffer wire materials is a smaller IBDr which means the two bracket planes crossed closer to the higher angle bracket. Burstone's predictive models for the moment dissociation point for stainless steel demonstrated a shift toward a geometry V for large deflections with wires that were free to slide and a shift toward a geometry III for large deflections with wires that were not free to slide. Our results show a shift toward a geometry III with a larger magnitude for stiffer wires.

With regard to the wire dimension, there was a significant difference in the moment dissociation point on the right bracket between all combinations except 0.012" and 0.016". It should be noted that fewer tests were performed on 0.012" wire due to the confounding variable of wire-bracket play with small gauge wires and close interbracket distances. The observed trend was a shift in the moment dissociation point toward a classically defined geometry III with smaller IBDr with larger dimension, and thus stiffer wires. This agrees with the shift seen in wire material.

Total angle (bracket A angle measured), demonstrate a significant difference in the moment dissociation point between all measured bracket A angles except 12° vs 24°. The emerging pattern shows that with both large and small deflections there is a shift in moment dissociation toward a geometry III with smaller IBDrs. The 6° data is shifted toward the geometry III, this is because variable combinations that were assigned the 6° bracket A angle were designated so due to material property constraints and an effort to avoid permanent deformation. All materials tested at 6° were SS or TMA, both

exhibiting higher stiffness and as we would predict, the moment dissociation point is shifted toward a geometry III. The shift toward a geometry III for the high angle measurements is a little less intuitive. All 48° measurements were taken on superelastic wires at 21 mm interbracket distance, exhibiting large deflections, low stiffness materials, over a long interbracket distance. It appears that with enough deflection stress a superelastic wire exceeds the threshold for a crystalline structure change from austenite to martensite, which produces an area within the wire with altered properties. We measured the forces and moments applied to bracket B while the wire was in a stationary "activated" position, deflected to fit into the geometry. In this state, the phase change alters the material properties of the beam in a way that shifts the moment dissociation point toward a geometry III.

Lastly, there was an observed shift in moment dissociation point toward a geometry III and smaller IBDrs with the shorter interbracket distance data. This concurs with the previous findings and reinforces the idea that the baseline moment dissociation point for linear materials does not occur at a geometry IV, but with larger deflections and less stiff materials, the moment dissociation point approaches a class IV geometry and an IBDr of 1/3, as in Burstone's simplified model.

The estimated effect size, Table 7, shows that the variables with the strongest effect on moment dissociation point are interbracket distance (51%) and total angle deflected (39%). These variables are directly related to wire stress and strain patterns and agree with the observation that wire deflection is a determining factor in the moment dissociation point. Additionally, we see that wire material (14%) and dimension (7%) have a smaller effect on the moment dissociation point. Wire material influences the

deflection pattern of the wire through both stiffness and when superelasticity occurs, both of which effect the moment dissociation point.

Table 7. Calculated variable effect size using $\boldsymbol{\eta_H^2 = \frac{H-k+1}{n-k}}$.

Variable	***Effect size***
Wire Material	0.1366
Wire Dimension	0.0694
Angle Bracket A	0.3943
Interbracket Distance	0.5118

H, Kruskal-Wallis H statistic; k, number of groups in variable; n, total number of observations

Conclusions

This study found an overall pattern of moment dissociation points which does not exactly coincide with the classical geometry IV, but rather, is shifted toward a geometry III where the intersection of the bracket planes (IBDr) was closer to the higher angle bracket than the classical 1/3 distance. The greatest shift away from a geometry IV was observed with stiffer wires and larger wire dimensions, smaller absolute angles of brackets, and shorter interbracket distances; the common factor between all these variables being smaller wire deflection. Configurations that produce larger wire deflection patterns demonstrate a moment dissociation point closer to that of Burstone and Koenig's theoretical geometry IV. The observed exception to this pattern lies with phase transforming pseudoelastic wires, because this effect biases the deformation pattern of the wire.

Clinically, the orthodontist should be aware of the force systems prescribed to each tooth when placing an ideal arch. To best ensure consistent force systems with minimal side effects, Burstone's geometries as modified by the data presented here are a quick and accurate method for determining the qualitative force system.

References

1. Burstone CJ, Koenig HA. Force systems from an ideal arch. *Am J Orthod*. 1974;65(3):270-289.

2. Marcotte MR. Prediction of orthodontic tooth movement. *Am J Orthod*. 1976.

3. Gatto E, Matarese G, Di Bella G, Nucera R, Borsellino C, Cordasco G. Load-deflection characteristics of superelastic and thermal nickel-titanium wires. *Eur J Orthod*. 2013;35(1):115-123. doi:10.1093/ejo/cjr103.

4. Ronay F, Kleinert W, Melsen B, Burstone CJ. Force system developed by V bends in an elastic orthodontic wire. *Am J Orthod Dentofacial Orthop*. 1989;96(4):295-301.

5. Burstone CJ, Choy K. *The Biomechanical Foundation of Clinical Orthodontics.* 15 ed.

6. Koenig HA, Burstone CJ. Analysis of generalized curved beams for orthodontic applications. *J Biomech*. 1974;7(5):429-435.

7. Isacson RJ, Lindauer SJ, Conley P. Responses of 3-dimensional arch wires to vertical v-bends: comparisons with existing 2-dimensional data in the lateral view. *Semin Orthod*. 1995;1(1):57-63.

8. Canales C, Larson M, Grauer D, Sheats R, Stevens C, Ko C-C. A novel biomechanical model assessing continuous orthodontic archwire activation. *Am J Orthod Dentofacial Orthop*. 2013;143(2):281-290. doi:10.1016/j.ajodo.2012.06.019.

9. Viecilli RF, Chen J, Katona TR, Roberts WE. Force system generated by an adjustable molar root movement mechanism. *Am J Orthod Dentofacial Orthop*. 2009;135(2):165-173. doi:10.1016/j.ajodo.2007.02.058.

10. Mulligan TF. Understanding wire/bracket relationships. *J Orofac Orthop*. 2002;63(6):493-508. doi:10.1007/s00056-002-0129-y.

11. Koenig HA, Burstone CJ. Force systems from an ideal arch--large deflection considerations. *Angle Orthod*. 1989;59(1):11-16. doi:10.1043/0003-3219(1989)059<0011:FSFAIA>2.0.CO;2.

12. Quick AN, Lim Y, Loke C, Juan J, Swain M, Herbison P. Moments generated by simple V-bends in nickel titanium wires. *Eur J Orthod*. 2011;33(4):457-460. doi:10.1093/ejo/cjq103.

13. Mallory DC, English JD, Powers JM, Brantley WA, Bussa HI. Force-deflection comparison of superelastic nickel-titanium archwires. *Am J Orthod Dentofacial Orthop*. 2004;126(1):110-112. doi:10.1016/S0889540604002100.

14. Fernandes DJ, Peres RV, Mendes AM, Elias CN. Understanding the shape-memory alloys used in orthodontics. *ISRN Dent*. 2011;2011(10):132408–6. doi:10.5402/2011/132408.

15. Gil FJ, Planell JA. Effect of copper addition on the superelastic behavior of Ni-Ti shape memory alloys for orthodontic applications. *Journal of Biomedical Materials Research Part A*. 1999;48(5):682-688. doi:10.1002/(SICI)1097-4636(1999)48:5<682::AID-JBM12>3.0.CO;2-M.

CHAPTER THREE

EXTENDED DISCUSSION

The most common technique in modern orthodontics is the straightwire technique with initial archwires consisting of relatively new superelastic materials. Brackets and bands are placed on each tooth in a position that is "ideal" and where in theory, when the archwire is completely straight and passive, the teeth will be in ideal occlusion. There are confounding anatomical and physiological factors that can alter the consistency of this technique, but in general, the teeth align to clinically acceptable positions.

Prior to the straight wire technique, the orthodontist would make bends in the archwire to position the tooth in the first, second, and third order. These bends produced the prescribed force system which would move the tooth from its initial position to the desired position. The belief with straight wire technique is that the correct force system will be applied to the tooth by virtue of the discrepancy between the ideal arch wire position and the position of the bracket slot into which it is deformed and placed. Two-attachment force systems can only be measured with force/moment load cells at each attachment simultaneously. Burstone and Koenig developed a qualitative system whereby the clinician can identify the category of force system based on the relative orientation of each bracket to the other and the interbracket plane. This system allows the clinician to prescribe a force system that is consistent with the desired movement of the individual tooth. If the clinician identifies that placing a straight wire between two attachments will produce a force system that is unfavorable or inconsistent, he or she can use an auxiliary appliance or alternate technique to prevent the predicted side effect from occurring.

The six geometries defined by Burstone and Koenig were done so in a study which did not describe the type of load cell used to collect data, nor were some details of the experimental process explained. In fact, it is reasonable to conclude that Burstone and Koenig came to their results through a combination of mathematical models and finite element analysis, whereby they entered the properties of a 0.016" round stainless steel orthodontic wire into formulae and calculated the force systems that would be produced. The author of this paper acknowledges that Burstone and Koenig's mathematical modeling of a two bracket system was not only elegant, it has allowed generations of astutue orthodontists to correctly predict force systems in complex appliances such as the straight wire technique. However, we want to be sure that these theoretical models are accurate, not only in a situation where actual wires and brackets are implemented, but also that they are still accurate with the advent of new materials in orthodontics.

This study aimed to test common variables in these two-attachement systems and compare with Burstone and Koenig's results as a method of updating and contributing to the system that has been previously described. The authors decided to focus on the most distinguishable characteristic in the six geometries described by Burstone and Koenig, the moment dissociation point. This point occurs, classically, when one bracket is the opposite direction and one half the magnitude of rotation of the adjacent bracket. When a stainless steel wire is inserted, according to Burstone and Koenig, the lesser angled bracket experiences no moment, only a single force, much like a cantilver. The clinical identification of this geometry is done by tracing a line through each bracket slot in space and connecting the two lines. The intersection point should occur at one third the interbracket distance, according to Burstone and Koenig.

The present study measured the location of this moment dissociation point with regard to the angle of the two brackets, and the location of the bracket plane intersection point, as can be readily identified clinically. Stainless steel, TMA, NiTi, and CuNiTi orthodointic wires of various cross sectional dimensions were compared at different interbracket distances and total angles. The goal was to identify any differences from the classic location of the moment dissociation point attributed to these variables.

The median experimental moment dissociation point for stainless steel occurred with the bracket plane intersection point occurring closer to one quarter the interbracket distance, rather than at the one third that is classically described. This means, that, in our experiment, which used force/moment load cells and actual orthodontic materials to simulate a clinical situation, we found a discrepancy between what Burstone's model would predict and where the actual moment dissociation point occurred. Trigonometry was used to calculate where the bracket planes intersected relative to the two brackets. To compare with Burstones model, we also calculated the classical geometry IV (moment dissociation point) intersection point from the theoretical angular relationship of the two brackets for purposes of having confirmation of our calculations and to recalculate the control data which Burstone produced. In doing so, it was discovered that the intersection point of the two bracket planes varied with the total angle of the brackets. This means that the intersection point when the left bracket was rotated 24 degrees counter clockwise and the right bracket was rotated 12 degrees clockwise deviated from the traditional one third relationship. When the angles were lowered to 12 and 6 degrees respectively, the result was closer to one third. It was discovered that the one third interbracket distance was a product of using a mathematical model with infinitely small

angles, a convergence point where the bracket slot planes came closer and closer to the interbracket plane while still maintaining the same geometry IV angular relationship. This means that one third is an exact relationship that would occur clinically, but rather an estimate calculated mathematically.

Our results indicate that the actual moment dissociation point occurs when the bracket slot planes intersect between one quarter and one third of the interbracket distance. We discovered two basic trends in our variables. The mechanism of both trends is that the experimental variables cause wire deformation pattern variations that affect the relationship of the two brackets where the moment dissociation point occurs. Wire deformation between two brackets is related to the wire material properties, the cross sectional area of the wire, the total angular difference and linear distance between the two brackets. The discovered trend was that stiffer wires, with larger cross sectional area, lower angle, and smaller interbracket distances had more of a shift away from the classical geometry IV and their moment dissociation point occurred with the intersection of the two bracket planes closer to the higher angle bracket. More elastic materials, with smaller cross sectional dimensions, larger angle and interbracket distances had moment dissociation points occurring closer to that of a classic geometry IV.

The exception to this trend occurred with superelastic wires that were deformed enough to introduce excessive stress into the wire which led to phase transformation and a change in the crystalline structure of the material, a process known as pseudoelasticity. A reduction in material stiffness occurs in this same area leading to more deformation and ultimately, a different deflection pattern. In such cases, we saw a shift in the intersection point of the bracket planes of the moment dissociation point toward the

classical one third interbracket distance of the geometry IV relative to similar data from linear elastic materials.

Along with the classical Burstone geometry categorizations, we can apply this new data to better predict the force system applied to teeth in a continuous arch wire. The prudent clinician inserting an archwire into a series of attachments can identify inconsistent force systems and predict side effects before they occur. When the a classical geometry IV is identified, applying the results of this study, we expect there to be a small moment on the attachment with the smaller angle. The experimental data of this study suggests that if a cantilever-like force system is desired, the interbracket plane intersection should occur closer to one fourth the interbracket distance with small deflections and stiff wires, whereas with larger deflections, and superelastic phase transforming wires, the intersection should occur nearer to the classic one third distance.

It is the hope of the author that more clinicians become aware of the force systems they prescribe each tooth during orthodontic treatment and are able to avoid unnecessary side effects and intermediate malocclusions that require more time and effort on the part of both the orthodontist and the patient. Using the classical Burstone geometry categorizations, modified by data presented in this paper, it is possible to clinically predict force systems on continuous archwires with modern orthodontic wires used for initial alignment.